Anal Bioanal Chem (2014) 406:3763–3772
DOI 10.1007/s00216-014-7770-3

RESEARCH PAPER

An amperometric uric acid biosensor based on chitosan-carbon nanotubes electrospun nanofiber on silver nanoparticles

Apon Numnuam · Panote Thavarungkul · Proespichaya Kanatharana

Received: 19 November 2013 / Revised: 20 February 2014 / Accepted: 16 March 2014 / Published online: 10 April 2014

Abstract A novel amperometric uric acid biosensor was fabricated by immobilizing uricase on an electrospun nanocomposite of chitosan-carbon nanotubes nanofiber (Chi–CNTsNF) covering an electrodeposited layer of silver nanoparticles (AgNPs) on a gold electrode (uricase/Chi–CNTsNF/AgNPs/Au). The uric acid response was determined at an optimum applied potential of −0.35 V vs Ag/AgCl in a flow-injection system based on the change of the reduction current for dissolved oxygen during oxidation of uric acid by the immobilized uricase. The response was directly proportional to the uric acid concentration. Under the optimum conditions, the fabricated uric acid biosensor had a very wide linear range, 1.0–400 μmol L^{-1}, with a very low limit of detection of 1.0 μmol L^{-1} (s/n=3). The operational stability of the uricase/Chi–CNTsNF/AgNPs/Au biosensor (up to 205 injections) was excellent and the storage life was more than six weeks. A low Michaelis–Menten constant of 0.21 mmol L^{-1} indicated that the immobilized uricase had high affinity for uric acid. The presence of potential common interfering substances, for example ascorbic acid, glucose, and lactic acid, had negligible effects on the performance of the biosensor. When used for analysis of uric acid in serum samples, the results agreed well with those obtained by use of the standard enzymatic colorimetric method (P> 0.05).

Keywords Uric acid biosensor · Chitosan-carbon nanotubes composite · Nanofiber · Electrospinning

Electronic supplementary material The online version of this article (doi:10.1007/s00216-014-7770-3) contains supplementary material, which is available to authorized users.

A. Numnuam (✉) · P. Thavarungkul · P. Kanatharana
Trace Analysis and Biosensor Research Center, Prince of Songkla University, Hat Yai, Songkhla 90112, Thailand
e-mail: anumnuam@gmail.com

A. Numnuam
e-mail: apon.n@psu.ac.th

A. Numnuam · P. Thavarungkul · P. Kanatharana
Center of Excellence for Innovation in Chemistry, Faculty of Science, Prince of Songkla University, Hat Yai, Songkhla 90112, Thailand

A. Numnuam · P. Kanatharana
Department of Chemistry, Faculty of Science, Prince of Songkla University, Hat Yai, Songkhla 90112, Thailand

P. Thavarungkul
Department of Physics, Faculty of Science, Prince of Songkla University, Hat Yai, Songkhla 90112, Thailand

Introduction

Uric acid (UA) in human blood and urine is the final product of purine metabolism by the liver [1, 2]. Abnormal UA levels reflect disorders of purine metabolism and serve as biomarkers for several diseases, for example gout, hyperuricemia, Lesch–Nyhan syndrome, and renal diseases [2, 3]. Electrochemical measurements, particularly with electrochemical biosensors based on the uricase enzyme electrode, are extremely attractive means of detection of UA because of several advantages, for example simplicity, ease of miniaturization, high selectivity and low cost [4].

A UA biosensor using uricase is based on the specific enzymatic oxidation of UA by oxygen to produce hydrogen peroxide, allantonin, and carbon dioxide. The reaction can be expressed as:

$$\text{Uric acid} + H_2O + O_2 \xrightarrow{\text{uricase}} \text{Allantonin} + H_2O_2 + CO_2$$

Amperometric detection can be based on determination of the H_2O_2 generated [5]. However, at the oxidation potential of

H_2O_2 other electroactive species, e.g., ascorbic acid (AA), could also be oxidized at the electrode. Alternatively a decrease in O_2 concentration can be measured, typically by use of a Clark-type O_2 electrode [6]. For detection of oxygen, there has recently been interest in the use of different catalysts, for example palladium [7], platinum nanoparticles [8], carbon nanotubes [9], and carbon nanofibers [10], for electroreduction of the oxygen. Silver nanoparticles (AgNPs) are comparatively inexpensive catalysts that have been evaluated and shown to be highly active in the O_2 reduction reaction [11, 12]. Thus, it is possible to use AgNPs as catalyst for detection of consumption of dissolved oxygen during enzymatic oxidation of UA.

Another important aspect of the development of a biosensor is the method of immobilization of the enzyme. To achieve high enzyme loading and catalytic efficiency, a support with a high surface area-to-volume ratio is desirable. Biocompatibility of the supporting material for enzyme immobilization is another important requirement, because if it can enable stable immobilization, reduce non-biospecific interactions, and retain the activity of the enzyme [13], this will be a huge advantage. For this purpose, chitosan (Chi) seems a promising candidate. Chitosan is a biopolymer that is biodegradable, nontoxic, and has abundant amino groups for enzyme immobilization by crosslinking. Fabrication in the form of a nanostructured electrospun polymeric nanofibrous membrane could provide a large surface area for the bound enzyme. The high porosity of this type of membrane can also improve the rate of mass transfer of the substrate to the active site of the enzyme [14–17]. To improve the electrical conductivity of the electrospun fiber, carbon nanotubes (CNTs) can be incorporated into the polymer matrix. Thus, an electrospun polymer–CNTs composite nanofiber that combined the advantages of conducting CNTs and a large specific surface area would be very effective. It has also been reported that the presence of CNTs in polymer nanofibers can enhance the activity of an enzyme [18]. To the best of our knowledge, there has been no report of the use of a AgNPs layer combined with an electrospun polymer–CNT composite in an enzymatic biosensor used to detect the current from reduction of dissolved oxygen catalyzed by AgNPs.

In this paper we report, for the first time, the development of a UA biosensor using an electrospun nanofibrous chitosan membrane containing CNTs (Chi–CNTsNF) as a supporting material for immobilization of uricase on an electrodeposited layer of AgNPs on a gold (Au) electrode (Uricase/Chi–CNTsNF/AgNPs/Au). The large surface area and good electron transfer of the electrospun Chi–CNTsNF nanocomposite enhanced the detection signal. The reduction current of the dissolved oxygen during oxidation of UA by the immobilized uricase was catalyzed by the presence of the AgNPs layer, and this helped avoid any interfering response. Optimization of conditions that might affect the sensing of the UA was investigated. The analytical performance of the Uricase/Chi–CNTsNF/AgNPs/Au electrode, e.g., its stability, linear range, limit of detection, Michaelis–Menten constant, specificity, and reproducibility, were evaluated. In addition, it was used to determine UA in human plasma samples.

Materials and methods

Materials

Chitosan (medium molecular weight) and uricase (Candida species, recombinant, expressed in *E. coli*, 4.9 units mg^{-1}) were from Sigma (Steinheim, Germany). Uric acid (≥98.0 %), anhydrous D-(+)-glucose (≥98.0 %), lactic acid (≥98.0 %), and glutaraldehyde (25 % solution) were from Fluka (Buchs, Switzerland). Silver nitrate was from Merck (Darmstadt, Germany), sodium dihydrogen orthophosphate and disodium hydrogen orthophosphate were from Ajax Finechem (New South Wales, Australia). Poly(vinyl alcohol) (PVA) (molecular weight 99,000) was from ChangChun Petrochemical (Taipei, Taiwan). MWCNTs (purity ≥95 %; average diameter 60–100 nm, length 2–5 μm) were from Shenzhen Nano-Technologies (Shenzhen, China) and were functionalized by use of 3:1 (*v*/*v*) concentrated H_2SO_4–HNO_3 before use. All other chemicals used were of analytical grade.

Preparation of the Chi–CNTsNF/AgNPs/Au electrode

Electrodeposition of AgNPs on to the Au electrode

A gold rod electrode (3.0 mm diameter, 99.99 % purity) was cleaned with piranha solution (3:1 H_2SO_4–H_2O_2) for 20 min, rinsed with distilled water, polished by use of alumina slurries (5, 1, and 0.3 μm, respectively), and etched electrochemically in 0.50 mol L^{-1} sulfuric acid for 25 cycles (0.1–1.5 V, scan rate 100 mV s^{-1}). Silver nanoparticles were electrodeposited on the gold electrode surface in 1.0 mmol L^{-1} $AgNO_3$ with 0.2 mol L^{-1} KNO_3 as supporting electrolyte at −0.40 V (vs. Ag/AgCl) for 30 s [19]. The morphology of the electrodeposited AgNPs on the gold electrode was observed by scanning electron microscopy (SEM, Quanta 400, FEI, The Netherlands).

Electrospun chitosan-CNTs nanofibrous membrane

The electrospun Chi–CNTsNF membrane was prepared by the method of Huang et al. [20], with a slight modification. Chitosan solution (3.0 % *w*/*w*) was prepared in acetic acid (90 %*v*/*v*) at room temperature with gentle stirring for 3 h. PVA solution (9.0 % *w*/*w*) was prepared in deionized water at 80 °C with gentle stirring for 1 h. The chitosan solution and PVA solution were then mixed in the volume ratio 40:60

(25 mL). MWCNTs (0.50 mg mL^{-1}) were then dispersed in this mixture with sonication for 8 h. Air bubbles were then removed by sonication for 30 min. This mixture (1.5 mL) was placed in a 3.0-mL plastic syringe with a 0.8 mm i.d. metal needle that was connected to the positive emitting electrode of a high-voltage power supply (Gamma High Voltage Research device, USA). The voltage ground was connected to an aluminium foil collector and the gold electrode was placed in the middle of the aluminium foil. Electrospinning was performed at 15 kV with a 15 cm distance between the needle tip and the electrode. The solution feed was driven by gravity and the electrostatic force that was generated during the spinning. Finally, the Chi–CNTsNF was obtained after treating the electrospun nanofibrous surface with 0.5 mol L^{-1} NaOH for 4 h to remove the PVA. The morphology of the electrospun nanofibers on the electrode was studied by scanning electron microscopy (SEM; Quanta 400; FEI, The Netherlands) and transmission electron microscopy (TEM; JEM-2010; Jeol, Japan).

Preparation of the uricase enzyme electrode (Uricase/Chi–CNTsNF/AgNPs/Au)

The amino groups (R-NH_2) of chitosan were activated by dropping 20 μL 5.0 % (*v*/*v*) glutaraldehyde in 10 mmol L^{-1} sodium phosphate buffer, pH 7.00, on top of the electrospun fibers and incubating at room temperature for 20 min to yield aldehyde groups. The electrode was then washed several times with sodium phosphate buffer to remove the excess glutaraldehyde. An appropriate amount of uricase enzyme in 5.0 μL was then placed on the electrode surface overnight at 4 °C for crosslinking between the amine group of the uricase and the amino group on the Chi–CNTsNF film. A Uricase/Chi–CNTsNF/AgNPs/Au electrode was obtained. When not in use, the modified electrode was stored at 4 °C in a closed container above 0.10 mmol L^{-1} sodium phosphate buffer, pH 7.00, and 0.02 % (*w*/*v*) sodium azide.

Electrochemical measurement

Electrochemical measurements were conducted with an Autolab PGSTAT 30 potentiostat–galvanostat (Metrohm Autolab, Utrecht, The Netherlands), with GPES 4.9 software for computer control. Cyclic voltammetric measurements were conducted with a three-electrode system consisting of the modified gold electrode as working electrode, an Ag/AgCl reference electrode, and a platinum wire as an auxiliary electrode. The responses to dissolved oxygen of the different modified electrodes without the immobilized uricase, i.e. ChiNF/Au, Chi–CNTsNF/Au, ChiNF/AgNPs/Au, and Chi–CNTsNF/AgNPs/Au, were studied. The cyclic voltammograms were recorded in 0.10 mol L^{-1} phosphate buffer solution, pH 7.00, with N_2 saturation (without dissolved O_2) and compared with those from the same solution with air added for 5 min (i.e. containing dissolved O_2).

For the amperometric UA detection, a flow-injection technique was applied. The Uricase/Chi–CNTsNF/AgNPs/Au modified electrode was inserted as the working electrode in a custom built three-electrode flow cell with a dead volume of 10 μL. A stainless steel tube was used as the auxiliary electrode and the outlet, and Ag/AgCl was used as reference electrode. They were connected to the Autolab. Standard UA solutions were injected through a six-port injection valve (Rheodyne, USA) into air-saturated phosphate buffer, and the UA was carried to the detection flow cell system by use of a peristaltic pump (Miniplus 3, Gilson, France). Amperometric measurements were performed by applying an appropriate potential that provided the highest change of the reduction current of dissolved oxygen during oxidation of UA by the immobilized uricase.

Optimization of the flow-injection amperometric UA biosensor

To obtain a flow-injection amperometric biosensor with high sensitivity, conditions that had a direct effect on UA detection, i.e., applied potential, amount of immobilized uricase, pH, concentration of phosphate buffer, flow rate, and sample volume, were optimized. The conditions were optimized by comparing the sensitivity (slope of the calibration curve) obtained for injected UA standard solutions, with three replicates for each concentration tested. The optimum of each condition was determined as a compromise between sensitivity and the time required for analysis.

Interference with biosensor response

Under the optimum conditions, potential common blood interferences, e.g., ascorbic acid (AA), glucose (Glu), and lactic acid (LA) at physiological concentrations were analyzed and the response were compared with that from UA. A mixture of UA standard (0.10 mmol L^{-1}), 0.10 mmol L^{-1} AA, 5.0 mmol L^{-1} Glu, and 0.50 mmol L^{-1} LA was tested. In addition, the response to mixtures of 0.10 mmol L^{-1} UA with each interfering compound at a concentration 100 times higher than that of the UA were also compared with that from 0.10 mmol L^{-1} UA alone.

Operational and storage stability

The operational stability was studied by repeatedly injecting 0.10 mmol L^{-1} UA into the flow system under the optimum conditions. For storage stability, an electrode was fabricated and kept in a closed container containing 0.10 mmol L^{-1} sodium phosphate buffer, pH 7.00, and 0.02 % (*w*/*v*) sodium azide. The enzyme electrode was used to detect UA (0.05–

0.20 mmol L^{-1}) at room temperature under the optimum conditions once a week for eight weeks.

Analysis of real samples

Blood plasma samples from Songklanagarind Hospital, Hat Yai, Thailand were analyzed. The effect of the matrix was first studied by comparing, by use of two-way ANOVA, the slope of the standard UA calibration curve with that of a calibration plot of plasma spiked with a series of uric acid concentrations. Samples diluted twentyfold were then tested with the developed system. The results obtained from the proposed UA biosensor were compared, by use of the Wilcoxon signed-rank test, with those from a standard hospital enzymatic colorimetric method.

Results and discussion

Characterization of the electrospun Chi–CNTsNF/AgNPs/Au

The surface morphology of the AgNPs and the electrospun Chi–CNTs nanofiber layers are shown in Fig. 1. The size of the globular structures of the layer of AgNPs formed after electrodeposition of 1.0 mmol L^{-1} $AgNO_3$ at −0.4 V (Ag/AgCl) for 30 s were between 22 and 34 nm (Fig. 1a). The electrospun Chi–CNTsNF on the AgNPs layer can be clearly seen in Figs. 1b–c. The nanofibers obtained were randomly orientated with relatively uniform diameters (mean 188± 15 nm). Under the TEM (Fig. 1d) it was observed that the CNTs were incorporated within the nanofiber. This fabricated Chi–CNTsNF/AgNPs/Au, with the porous three-dimensional structure of the electrospun nanofibers, should provide a favorable support for the immobilized enzyme and the ability to enhance electron transfer.

Electrochemical properties of the modified electrodes

Different modified electrodes i.e. ChiNF/Au, Chi–CNTsNF/Au, ChiNF/AgNPs/Au, and Chi–CNTsNF/AgNPs, without immobilized uricase were used to measure dissolved oxygen. Figure 2 shows the cyclic voltammetric behavior of these electrodes. In the absence of O_2, no reduction peak was observed (curve a). When O_2 was added, the electrochemical reduction peak for dissolved oxygen was clearly observed for the ChiNF/AgNPs/Au (Fig. 2c, curve b) and the Chi–CNTsNF/AgNPs/Au (Fig. 2d, curve b) with the reduction peak center at −0.4 V. For the ChiNF/Au (Fig. 2a, curve b) and Chi–CNTsNF/Au (Fig. 2b, curve b) no

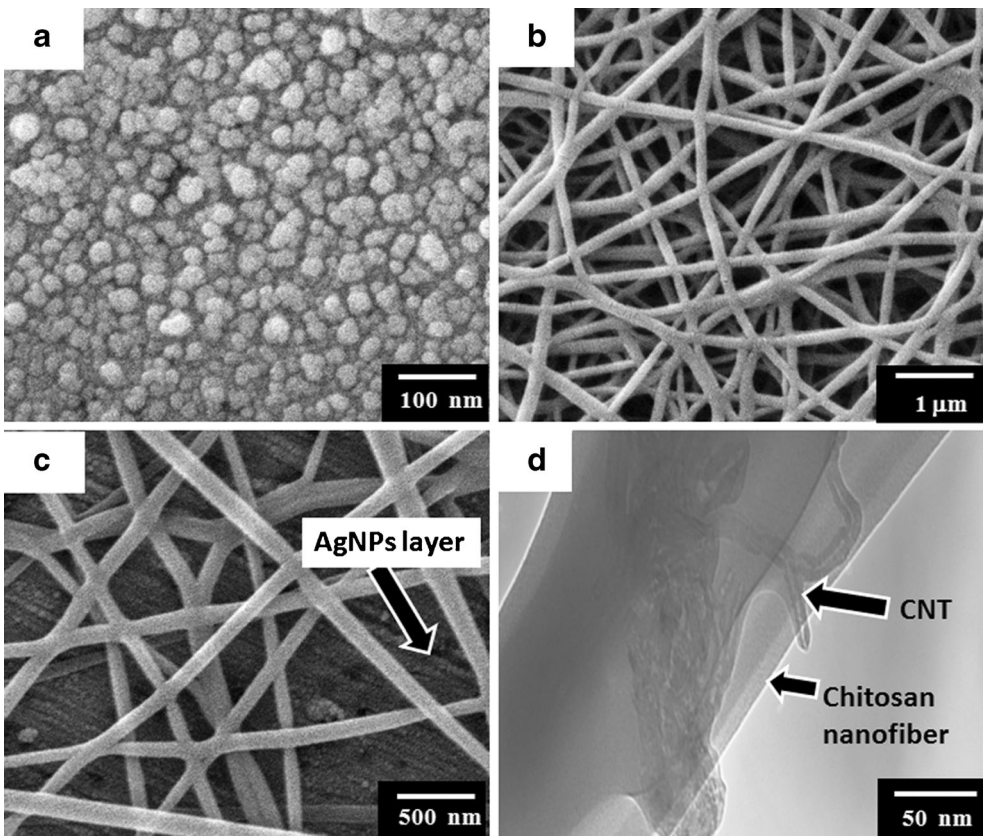

Fig. 1 SEM images of electrode surface modified with AgNPs, at ×50,000 (**a**) and Chi–CNTsNF/AgNP, at ×10,000 (**b**) and ×30,000 (**c**). TEM image of Chi–CNTsNF at ×200,000 (**d**)

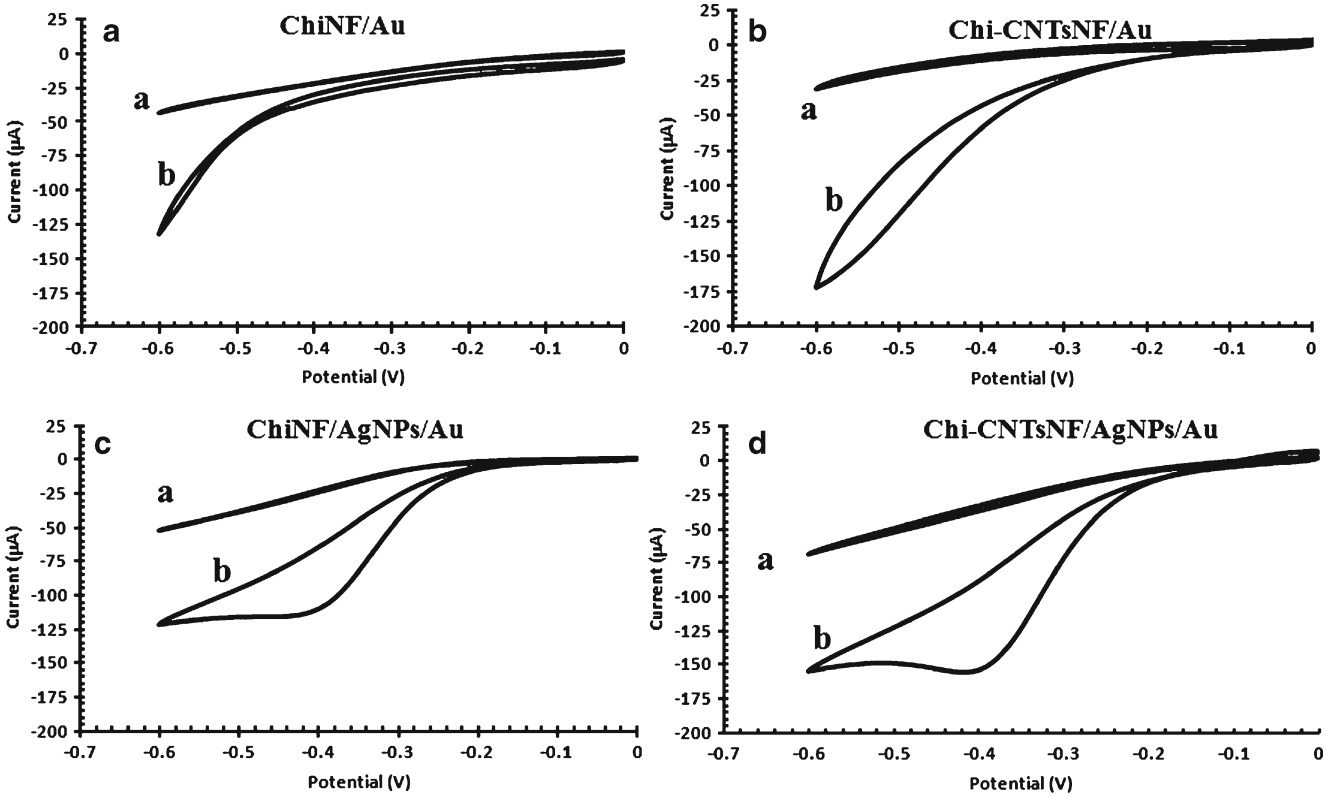

Fig. 2 Cyclic voltammograms obtained from (**a**) ChiNF/Au, (**b**) Chi–CNTsNF/Au, (**c**) ChiNF/AgNPs/Au, and (**d**) Chi–CNTsNF/AgNPs/Au in 0.1 mol L^{-1} N_2-saturated phosphate buffer solution (pH 7.00) (*curve a*) and phosphate buffer solution containing dissolved O_2 (*curve b*). The scan rate was 0.05 V s^{-1}

reduction peak for O_2 was observed. These results clearly indicated that the catalytic electroreduction of oxygen occurred in the presence of the AgNPs layer. The reduction current obtained from Chi–CNTsNF/AgNPs/Au (Fig. 2d) was also much higher than that from the ChiNF/AgNPs/Au (Fig. 2c). The increased current was because of the presence of the CNTs, which had a large surface-to-volume ratio and helped to enhance the efficiency of electron transfer between the nanofiber membrane and the electrode. Therefore, the Chi–CNTsNF/AgNPs/Au electrode was further investigated with immobilized uricase.

Optimization of the flow-injection amperometric UA biosensor

The electrochemical response of the Uricase/Chi–CNTsNF/AgNPs/Au electrode to UA was optimized by use of amperometry with a flow-injection system. The effect of some conditions were as follows.

Applied potential

The operating voltage is one of the conditions most critical amperometric response and selectivity. From the cyclic voltammetry response of the Chi–CNTsNF/AgNPs/Au electrode to dissolved oxygen, the reduction peak current occurred between −0.50 and −0.20 V (Fig. 2d, curve b). Therefore, potentials of −0.50, −0.45, −0.40, −0.35, −0.30 and −0.20 V were used for amperometric detection of UA (0.05–0.2 mmol L^{-1}). The best sensitivity was obtained at −0.35 V (Electronic Supplementary Material Fig. S1), so all further studies were carried out at −0.35 V.

Amount of uricase

Increasing the amount of uricase on the sensing electrode should increase the consumption of oxygen during the process of oxidation of UA by the enzyme, leading to a decrease of the oxygen reduction current, i.e. the change of reduction current will increase. Immobilized uricase from 5 to 15 units was tested and the sensitivity increased from 6.0±0.4 to 15.5±0.5 μA $mmol^{-1}$ L (Electronic Supplementary Material Fig. S2). The increase in enzyme loading on the electrode resulted in an increase of the number of active sites of the enzyme on the electrode, which could catalyze more substrate. In contrast uricase loading at 20 and 25 units reduced the sensitivity, probably because of an increase in electron-transfer resistance as film thickness increased [21]. Therefore, 15 units of uricase was chosen for all further fabrications.

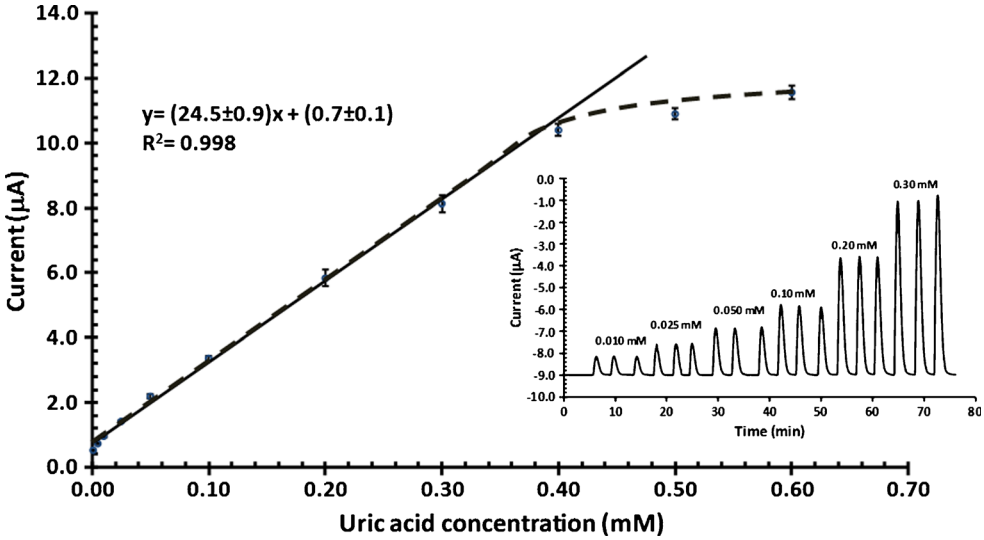

Fig. 3 Calibration curve for the fabricated uric acid biosensor and (*inset*) an example of the current response for different concentrations of uric acid in flow-injection analysis

Buffer concentration and pH

Because the enzymatic catalyst is pH and ionic strength-sensitive [22], the concentration and pH of the sodium phosphate buffer were optimized simultaneously by evaluating the highest sensitivity at every combination of concentration (0.10, 0.20, and 0.30 mol L^{-1}) and pH (6.00, 6.50, 7.00, 7.50, and 8.00). The results clearly showed that the highest sensitivity for detection of UA (20.5±0.4 μA $mmol^{-1}$ L) was obtained with 0.20 mol L^{-1} sodium phosphate buffer, pH 7.50 (Electronic Supplementary Material Fig. S3) which is slightly lower than that for use of the free enzyme (pH 8.00) [23]. The decrease in the optimum pH after immobilization might be because of a change of uricase conformation that might alter the active site therefore reduce the enzymatic activity. Another reason might be the structure of UA, because UA can have several forms depending on pH. Because the pK_a values of UA are 5.4 and 9.8 [24], acid dissociation of UA possibly affected sensitivity when the pH was too high [6].

Flow rate and sample volume

The effect of flow rate and sample volume were optimized simultaneously by use of 0.05–0.20 mmol L^{-1} UA with every combination of sample volume (250, 300, 350, and 400 μL) and flow rate (250, 300, 400, 500, and 600 and 700 μL min^{-1}). The sensitivity increased with increasing flow rate and sample volume until a flow rate of 500 μL min^{-1} and 300 μL sample volume, where the highest sensitivity (24.2± 0.5 μA $mmol^{-1}$ L) was obtained (Electronic Supplementary Material Fig. S4) with a fast response time (3.0 min). This was because the increase in the flow rate and the sample volume provided more efficient mass transport of the substrate to the porous Chi–CNTsNF membrane-modified electrode. If the flow rate was too fast, however, this did not enable enough contact time between the target analyte and the immobilized enzyme, so sensitivity decreased. Therefore, a 500 μL min^{-1} flow rate and 300 μL sample volume were chosen.

In summary, the optimum conditions were: applied potential −0.35 V, 15 units of immobilized uricase, 0.20 mol L^{-1} phosphate buffer, pH 7.50, for the carrier and sample buffer solution, flow rate 500 μL min^{-1}, and sample volume 300 μL.

Performance of the modified electrode

Linear dynamic range and limit of detection

The change of the reduction current for dissolved oxygen increased linearly with increasing UA concentration between 1.0 μmol L^{-1} and 0.40 mmol L^{-1} with a correlation coefficient of 0.998 (Fig. 3). The detection limit, 1.0 μmol L^{-1}, was determined from the lowest concentration of UA that provided a signal three times higher than that of the background noise (s/n=3).

The apparent Michaelis–Menten constant (K_M^{app}), a reflection of enzymatic affinity, can be calculated by use of the Lineweaver–Burk equation [25]:

$$\frac{1}{i_{SS}} = \frac{1}{i_{\max}} + \frac{K_M^{app}}{i_{\max} \text{ x } c}$$

where i_{ss} is the steady-state current after addition of substrate, i_{max} is the maximum current measured under saturated substrate conditions, and c is the bulk concentration of the substrate. The K_M^{app} value was calculated to be 0.21 mmol L^{-1}. This low value of K_M^{app} indicated high affinity of the

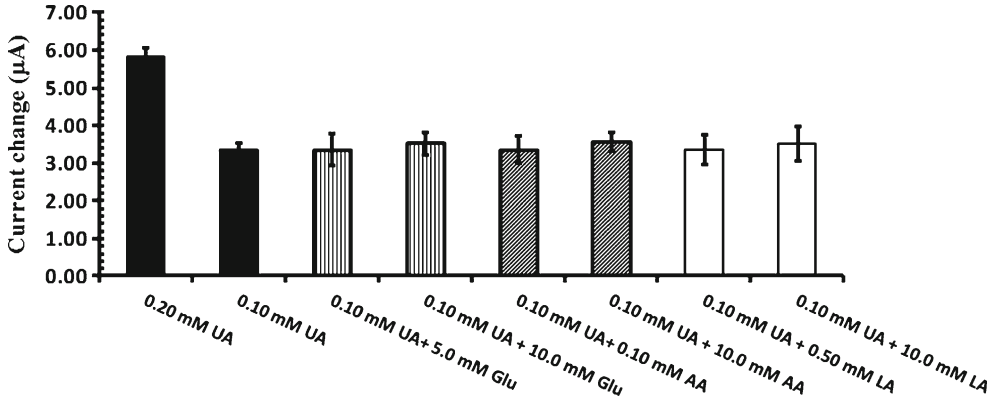

Fig. 4 Results from a study of the selectivity of the fabricated biosensor after addition of possible interfering substances at physiological levels, glucose (5.0 mmol L^{-1}), ascorbic acid (0.10 mmol L^{-1}), lactic acid (0.50 mmol L^{-1}), and 10.0 mmol L^{-1} of each substance in a solution also containing 0.10 mmol L^{-1} uric acid

immobilized uricase for UA, which might be because of enhanced diffusion of UA through the Chi–CNTsNF/AgNPs-modified electrode.

Interferences with biosensor response

As shown in Fig. 4, the current response to mixtures of 0.10 mmol L^{-1} UA with interferences at the physiological level and at concentrations 100 times higher than that of UA were not significantly different from the response to 0.10 mmol L^{-1} UA standard. This shows that this biosensor enables highly selective quantification of uric acid in blood plasma as a real sample.

Operational and storage stability

The response of the modified electrode showed operational stability was excellent for up to 205 injections (Fig. 5a) with a relative standard deviation (RSD) of 3.2 %. After 205 injections, the current response remained at 98 % and decreased to 90 % after 215 injections. The low RSD was indicative of good reproducibility of the modified electrode in response to UA. From observation of the electrode at the end of the study, the sensing surface has lost some of the Chi–CNT nanofibrous membrane that acted as support for the immobilized uricase, the rapid decrease of the response after 205 injections was most likely the result of this loss. The storage stability is

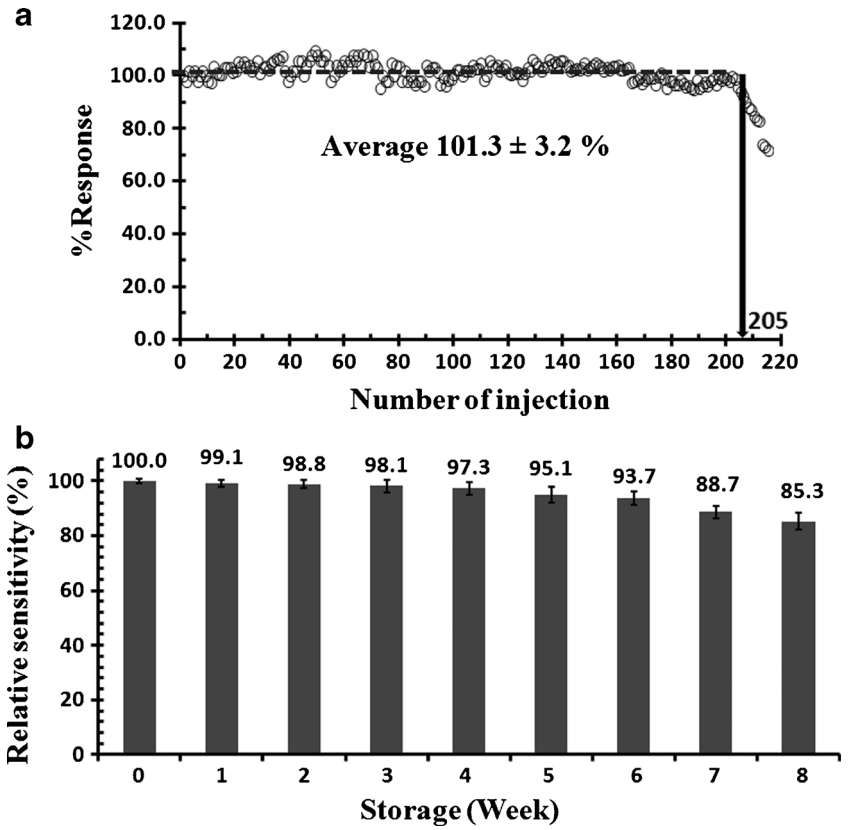

Fig. 5 Operational (**a**) and storage (**b**) stability of the Uricase/Ch-CNTsNF/AgNPs/Au biosensor

shown in Fig. 5b. The enzyme electrode had excellent storage stability, retaining more than 90 % of the initial sensitivity after storage for up to six weeks. After eight weeks, 85 % of the sensitivity still remained. This excellent operational and storage stability were made possible by the chitosan and the carbon nanotube nanocomposite fibrous membrane used as the supporting material. The structure of the Chi–CNTsNF membrane was a combination that was both chemically and mechanically stable and was ideal for immobilization of the enzymes. The carbon nanotube-composite nanofiber has been reported to be an effective additive for avoiding the decrease of activity resulting from immobilization of the enzyme and has been shown to enhance enzyme activity [18]. Moreover, the Coulombic interaction between the negatively charged groups of uricase and the positive amino group of the Chi–CNTs supporting material also led to formation of a more rigid and stable structure.

Reproducibility

The reproducibility of the process used for fabrication for the biosensor was investigated. Six electrodes were fabricated on different days and used to measure a series of UA concentrations of 0.05–0.2 mmol L^{-1}. The sensitivity of the six electrodes was 24.2±0.1, 24.7±0.2, 24.4±0.2, 24.5±0.2, 24.8±0.2, and 25.0±0.3 μA. $mmol^{-1}$ L. The relative standard deviation (RSD) of the sensitivity of the six electrodes was 1.45 %, revealing a good reproducibility in the fabrication of the biosensors.

The analytical performance of the Uricase/Chi–CNTsNF/AgNPs/Au electrode and those other modified electrodes for uric acid amperometric biosensors are shown in Table 1. Although the linear range of this fabricated biosensor may not be as wide as in some previous reports [6, 23, 26, 27], it is sufficient for direct detection of UA in diluted human plasma samples (normal physiological range 0.13–0.46 mmol L^{-1}, and higher for many diseases, for example gout, hyperuricemia, and kidney disease [28]). The limit of detection, 1.0 μmol L^{-1}, was better than in most reports [6, 23, 26, 27, 29] except for the modified electrode with Uricase/PPy-Fc/Pt [30]. However, this 1.0 μmol L^{-1} LOD is still much lower than the level of UA in plasma samples and should not pose any difficulty in the detection. The Michaelis–Menten constant (K_M^{app}), used to indicate the affinity of the immobilized enzyme for uric acid, after this method immobilization was lower than for most earlier uric acid biosensors based on different types of supported enzyme [6, 26, 27, 30, 31]. In addition, the storage stability of this fabricated biosensor was comparable with or better than that in some previous work [26, 27, 29, 31, 32]. The result indicated that Chi–CNTsNF/AgNPs was able to maintain the activity of the immobilized uricase with high affinity. The good analytical performance of this fabricated enzyme electrode is most likely because of the large surface area, good electron transfer of the electrospun Chi–CNTsNF nanocomposite, and the presence of AgNPs layer. It had excellent electrocatalytic activity in electroreduction of dissolved oxygen and can enhance the detection response.

When considering enzyme electrode fabrication processes, although the enzyme electrode in this work was modified in three steps, compared with previous one-step [32] and two-step [29] modifications, it resulted in much better stability, six weeks compared with 15 days [29] and 21 days [32], probably because the enzyme immobilized on these two electrodes were either by adsorption [29] or entrapment [32], hence the enzyme is easily lost, so their stabilities were much less.

Table 1 Comparison of the performance of the proposed uric acid biosensor and other reported amperometric uric acid biosensors based on modified electrodes

Structure of biosensor	Detection principle	K_M (mmol L^{-1})	Linear range (μmol L^{-1})	LOD (μmol L^{-1})	Stability	Ref.
Uricase/egg shell membrane/ O_2 electrode	O_2	0.33	4.0-640	2.0	89 %,3 months	[6]
Uricase/PBNPs/MWCNT/ PANI/Au	H_2O_2	0.055	5.0-800	5.0	63 % 400 injection or 210 days	[23]
Uricase/PPy-Fc/Pt	H_2O_2	0.44	1.0-50	0.5	51 %, 7 weeks	[30]
Uricase/AuNPs/MWCNT/Au	H_2O_2	0.50	10-800	10	75 %, 45 days	[26]
Uricase/PANI-PPy/Au	H_2O_2	1.57	2.5-85	1.0	80 %, 4 weeks	[31]
Uricase/AuNPs/ Amino acid/ Au	H_2O_2	1.78	20-2500	7.0	90 %, 30 days	[27]
Uricase/PBNPs/SPE	H_2O_2	NR	30-300	10	90 %, 15 days	[29]
Uricase-PS membrane/Au	O_2	NR	5-105	NR	87 %, 21 days	[32]
Uricase/Chi–CNTsNF/ AgNPs/Au	O_2	0.21	1.0-400	1.0	98 % 205 injections 90 % 215 injections 90 %, 6 weeks	This work

Chi, chitosan; NPs, nanoparticles; PBNPs, Prussian blue nanoparticles; PPy, polypyrrole; Fc, ferrocene: Pt, platinum; MWNT, multiwalled carbon nanotubes; CNTs, carbon nanotubes: Chi–CNTsNF, Chitosan-carbon nanotubes nanofiber: SPE, Screen printed electrode: PS membrane, polystyrene membrane; NR, not reported

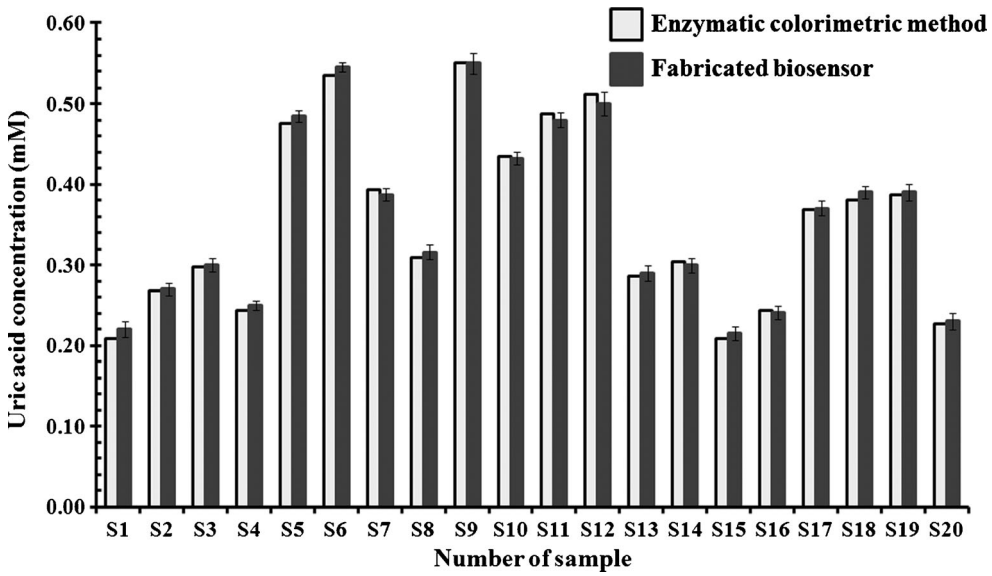

Fig. 6 Comparison of the analytical results obtained by use of the fabricated biosensor and the hospital standard method

When the two detection principles, detection of H_2O_2 and O_2 are compared, detection based on H_2O_2 is usually affected by ascorbic acid, a common blood interference [26]. To reduce such interference a mediator is required [23, 29, 30]. For detection of the O_2 concentration in this work, the effect of common blood interferences (ascorbic acid, glucose, and lactic acid) can be avoided (Fig. 4). Although the analysis required a constant level of O_2, in a flow system this steady level of oxygen can be achieved simply by adding an air-pump to provide air-saturated phosphate buffer as background solution.

Compared with the commercial uric acid test strips now available from many companies, although the test strip is convenient and can be used to detect uric acid in whole blood, it can be used only once and so will be more expensive when a large number of samples must be tested. For the clinical laboratories, the current standard method is the enzymatic-colorimetric method based on uricase and peroxidase, this test, also, is performed not on whole blood, but on plasma samples. Although this method is widely used in routine analysis, because of its simplicity, sensitivity, and specificity, the cost of uricase and peroxidase, used as free enzymes in each test, is high, especially for a large number of samples. In this latter case the method described in this report would be more efficient and cost effective, because one electrode can be used up to approximately 200 times (Fig. 5a).

Analysis of real samples

Blood plasma samples were obtained from Songklanagarind Hospital, Hat Yai, Thailand. The matrix effect was first studied by comparing the biosensor response to UA standard with that to a mixture of UA standard and a blood sample. UA standards at concentrations of 0.20, 0.30, 0.40, 0.50, and 0.60 mmol L^{-1} prepared in 100 μL 0.20 mol L^{-1} phosphate buffer, pH 7.50, were mixed with 100 μL blood plasma and adjusted to 2,000 μL with buffer to achieve 20 fold dilution. The final concentrations of UA in the mixtures were 0.010, 0.015, 0.020, 0.025, and 0.030 mmol L^{-1}, respectively. There was no significant difference ($P>0.05$) between the sensitivity for the mixed samples and the UA standard. Therefore, human plasma samples were diluted 20-fold before analysis by use of the biosensor.

When twenty blood plasma samples were analyzed by use of the biosensor UA concentrations ranged from 0.21–0.54 mmol L^{-1} with an RSD ($n=3$) between 2.1 and 4.5 %. When these results were compared with the those from the standard enzymatic colorimetric method (Fig. 6), by use of the Wilcoxon signed-rank test, the differences between the two methods were not significant ($P>0.05$).

To further validate the amperometric UA detection system, recovery of UA from blood samples spiked with UA at different concentrations (0.20, 0.30, 0.40, 0.50 and 0.60 mmol L^{-1}) was tested. After 20-fold dilution, the responses obtained were used to calculate the concentration from the standard calibration plot. Recovery was from 97 % to 105 % with RSD ($n=3$) between 2 and 5 % (Electronic Supplementary Material Table S1).

Conclusions

A novel UA biosensor based on Uricase/Chi–CNTsNF/AgNPs/Au has been prepared and its properties studied. The biosensor measured uric acid concentrations via amperometric detection of the reduction of dissolved oxygen, consumed in the process of oxidation of UA by uricase. Modification of the electrode surface with a layer of AgNPs resulted in excellent

electrocatalytic activity in electroreduction of the dissolved oxygen. The fabricated biosensor had a very low detection limit, a wide linear range, with satisfactory selectivity and reproducibility and excellent stability. The fabricated UA biosensor also had a low Michaelis–Menten constant and the values measured for real samples agreed with those obtained by use of the standard hospital method. This fabricated Chi–CNTsNF/AgNPs/Au modified electrode could be used as a supporting material for other biosensor applications based on oxidase enzymes.

Acknowledgements This work was supported by the Office of the Higher Education Commission, the Thailand Research Fund (TRF) grant no. MRG 5380269, and the Faculty of Science, Prince of Songkla University. Partial support was received from the Trace Analysis and Biosensor Research Center (TAB-RC), the Center of Excellence for Innovation in Chemistry (PERCH-CIC), and the Office of the Higher Education Commission. The authors thank Dr Brian Hodgson and Asst. Prof. Dr. Chittanon Buranachai, Prince of Songkla University, Hat Yai, Songkhla, Thailand, for assistance with the English.

References

1. Huang SH, Shih YC, Wu CY, Yuan CJ, Yang YS, Li YK, Wu TK (2004) Detection of serum uric acid using the optical polymeric enzyme biochip system. Biosens Bioelectron 19:1627–1633
2. Zhang Y, Buchholz F, Muyrers JPP, Francis Stewart A (1998) A new logic for DNA engineering using recombination in escherichia coli. Nat Genet 20:123–128
3. Ren W, Luo HQ, Li NB (2006) Simultaneous voltammetric measurement of ascorbic acid, epinephrine and uric acid at a glassy carbon electrode modified with caffeic acid. Biosens Bioelectron 21:1086–1092
4. Özcan A, Şahin Y (2010) Preparation of selective and sensitive electrochemically treated pencil graphite electrodes for the determination of uric acid in urine and blood serum. Biosens Bioelectron 25: 2497–2502
5. Kan J, Pan X, Chen C (2004) Polyaniline-uricase biosensor prepared with template process. Biosens Bioelectron 19:1635–1640
6. Zhang Y, Wen G, Zhou Y, Shuang S, Dong C, Choi MMF (2007) Development and analytical application of an uric acid biosensor using an uricase-immobilized eggshell membrane. Biosens Bioelectron 22:1791–1797
7. Lin Y, Cui X, Ye X (2005) Electrocatalytic reactivity for oxygen reduction of palladium modified carbon nanotubes synthesized in supercritical fluid. Electrochem Commun 7:267–274
8. Cui HF, Ye JS, Zhang WD, Wang J, Sheu FS (2005) Electrocatalytic reduction of oxygen by a platinum nanoparticle/carbon nanotube composite electrode. J Electroanal Chem 577:295–302
9. Ye JS, Wen Y, Zhang WD, Cui HF, Gan LM, Xu GQ, Sheu FS (2004) Application of multi-walled carbon nanotubes functionalized with hemin for oxygen detection in neutral solution. J Electroanal Chem 562:241–246
10. Wu L, Zhang X, Ju H (2007) Amperometric glucose sensor based on catalytic reduction of dissolved oxygen at soluble carbon nanofiber. Biosens Bioelectron 23:479–484
11. Singh P, Buttry DA (2012) Comparison of oxygen reduction reaction at silver nanoparticles and polycrystalline silver electrodes in alkaline solution. J Phys Chem C 116:10656–10663
12. Wu S, Zhao H, Ju H, Shi C, Zhao J (2006) Electrodeposition of silver–DNA hybrid nanoparticles for electrochemical sensing of hydrogen peroxide and glucose. Electrochem Commun 8:1197–1203
13. Sadana A (1992) Protein adsorption and inactivation on surfaces. Influence of heterogeneities. Chem Rev 92:1799–1818
14. Lee KH, Ki CS, Back DH, Kang GD, Ihm DW, Park YH (2005) Application of electrospun silk fibroin nanofibers as an immobilization support of enzyme. Fibers Polym 6:181–185
15. Patel AC, Li S, Yuan JM, Wei Y (2006) In situ encapsulation of horseradish peroxidase in electrospun porous silica fibers for potential biosensor applications. Nano Lett 6:1042–1046
16. Xie J, Hsieh YL (2003) Ultra-high surface fibrous membranes from electrospinning of natural proteins: casein and lipase enzyme. J Mater Sci 38:2125–2133
17. Ye P, Xu ZK, Wu J, Innocent C, Seta P (2006) Nanofibrous poly(acrylonitrile-co-maleic acid) membranes functionalized with gelatin and chitosan for lipase immobilization. Biomaterials 27:4169–4176
18. Wang Z-G, Ke B-B, Xu Z-K (2007) Covalent immobilization of redox enzyme on electrospun nonwoven poly(acrylonitrile-co-acrylic acid) nanofiber mesh filled with carbon nanotubes: a comprehensive study. Biotechnol Bioeng 97:708–720
19. Chen Y-C, Young RJ, Macpherson JV, Wilson NR (2007) Single-walled carbon nanotube networks decorated with silver nanoparticles: a novel graded SERS substrate. J Phys Chem C 111:16167–16173
20. Huang X-J, Ge D, Xu Z-K (2007) Preparation and characterization of stable chitosan nanofibrous membrane for lipase immobilization. Eur Polym J 43:3710–3718
21. Liu Y, Qu X, Guo H, Chen H, Liu B, Dong S (2006) Facile preparation of amperometric laccase biosensor with multifunction based on the matrix of carbon nanotubes–chitosan composite. Biosens Bioelectron 21:2195–2201
22. Portaccio M, Di Martino S, Maiuri P, Durante D, De Luca P, Lepore M, Bencivenga U, Rossi S, De Maio A, Mita DG (2006) Biosensors for phenolic compounds: the catechol as a substrate model. J Mol Catal B Enzym 41:97–102
23. Rawal R, Chawla S, Chauhan N, Dahiya T, Pundir CS (2012) Construction of amperometric uric acid biosensor based on uricase immobilized on PBNPs/cMWCNT/PANI/Au composite. Int J Biol Macromol 50:112–118
24. Simic MG, Jovanovic SV (1989) Antioxidation mechanisms of uric acid. J Am Chem Soc 111:5778–5782
25. Lehninger DN, Cox MC (2008) Lehninger principles of biochemistry, 4th edn. WH Freeman, New York
26. Chauhan N, Pundir CS (2011) An amperometric uric acid biosensor based on multiwalled carbon nanotube-gold nanoparticle composite. Anal Biochem 413:97–103
27. Liu Y, Yuan M, Liu L, Guo R (2013) A facile electrochemical uricase biosensor designed from gold/amino acid nanocomposites. Sensors Actuators B 176:592–597
28. Raj CR, Ohsaka T (2003) Voltammetric detection of uric acid in the presence of ascorbic acid at a gold electrode modified with a self-assembled monolayer of heteroaromatic thiol. J Electroanal Chem 540:69–77
29. Piermarini S, Migliorelli D, Volpe G, Massoud R, Pierantozzi A, Cortese C, Palleschi G (2013) Uricase biosensor based on a screen-printed electrode modified with Prussian blue for detection of uric acid in human blood serum. Sensors Actuators B 179:170–174
30. Çete S, Yaşar A, Arslan F (2006) An amperometric biosensor for uric acid determination prepared from uricase immobilized in polypyrrole film. Artif Cells Blood Substit Biotechnol 34:367–380
31. Arslan F (2008) An amperometric biosensor for uric acid determination prepared from uricase immobilized in polyaniline-polypyrrole film. Sensors 8:5492–5500
32. Wang X, Hagiwara T, Uchiyama S (2007) Immobilization of uricase within polystyrene using polymaleimidostyrene as a stabilizer and its application to uric acid sensor. Anal Chim Acta 587:41–46